

DSC and IR methods for determination of accessibility of cellulosic coir fibre and thermal degradation under mercerization

D N Mahato^{1,a}, B K Mathur² & S Bhattacharjee²

¹Department of Physics, Tata College Chaibasa, Kolhan University, Chaibasa 833 201, India

²Department of Physics and Meteorology, Indian Institute of Technology, Kharagpur 721 302, India

Received 21 September 2011; revised received and accepted 5 December 2011

The accessibility of alkali treated coir fibre has been studied using differential scanning calorimetry and infrared spectroscopy. The lattice transformation in ligno-cellulosic coir fibre is restricted. The crystallinity of the fibre decreases with the increase in NaOH concentration. These studies appear to support the three phase model.

Keywords : Amorphous material, Coir fibre, Crystalline structure, Mercerization, Semi crystalline structure, Three phase model, Thermal stability

1 Introduction

Coir is a ligno-cellulosic fruit fibre. In the natural fibre, crystalline cellulose is embedded in the amorphous lignin which provides mechanical strength to the fibre participating in the stress transfer¹. The delignification of the natural fibre ruptures the fibre and therefore, unlike other fibres, it is used in the natural form. Sodium hydroxide (NaOH) treatment to cellulosic fibres increases the tensile strength, improving elasticity, lustre and dyeing properties, which is known as mercerization. Cellulose is an important structural component of coir fibre, existing as long fibres composed of smaller structural units called microfibrils, which, in turn, consists of aggregate of elementary fibrils. Although many models have been proposed to explain the structure of cellulose, no model can account for all the observed properties of the microfibrils². Nevertheless, all such theories assume the existence of two distinctly different regions within the microfibril. One is highly ordered cellulose molecules called the crystalline regions, and the other of less ordered cellulose molecules called the amorphous region. There are probably no sharp boundaries between both the areas, but there is rather a gradual transition from the highly crystalline regions to the completely amorphous areas. Mitra and Mukherjee³ proposed a three phase model

paracrystalline. The cellulosic materials from all natural sources (plant, fruit and wood) have the same cellulose. Crystalline structure is called cellulose I or native cellulose. Most aqueous reagents penetrate only the amorphous areas of cellulose fibres. Therefore, these amorphous or noncrystalline regions are called the accessible regions of cellulose. Hence, the concepts of crystallinity and accessibility are closely related. Cellulose molecular cohesion is due to large number of hydroxyl groups forming intramolecular hydrogen bonds between adjacent glucose units of the chain and intermolecular hydrogen bonds between different chains. These hydrogen bonds are responsible for the fibrillar and crystalline structure of cellulose⁴. However, a considerable number of free hydroxyl groups is also present in cellulose fibres, primarily in the noncrystalline regions of cellulose. Therefore, as the capacity of cellulose fibres for water absorption depends largely on the availability of free hydroxyl groups, it is generally considered that water sorption occurs almost entirely in the amorphous regions of cellulose, neglecting the free hydroxyl groups that may be present on the surface of the crystallites⁵. For highly crystalline celluloses, water adsorbed on crystal surface cannot be neglected. The crystal surfaces for highly crystalline materials contribute significantly to the cellulose accessibility. In our study, however, we concentrated on more amorphous materials, for which the assumption for relatively

^aCorresponding author.
E-mail: dn.mahato08@yahoo.com

little water adsorbed on crystal surface is a good approximation. XRD method of determination of crystallinity suffers from the difficulty arises due to uncertainty or to the shape of the amorphous background in the X-ray diffraction measurements. It is pertinent to consider the effect of a phase of intermediate order. Crystallite orientation also affects XRD. Coir fibre cannot be prepared as purely amorphous with alkali treatment. Therefore, a qualitative change in the crystallinity may be obtained from the DSC thermogram which is corroborated by the IR method of determination of crystallinity. In this work, the accessibility of alkali treated coir fibre has been studied using differential scanning calorimetry and infrared spectroscopy.

2 Theoretical Consideration

The method reported by Bertran and Dale⁵ has been used to determine the accessibility by DSC. The dehydration endothermic peak area (energy required) is the indirect method of measurement of accessibility of amorphous region. Therefore, crystallinity (CA) is defined as:

$$CA\% = \frac{\Delta H_o - \Delta H_s}{\Delta H_o}$$

where ΔH_o is the heat required to dehydrate the standard cellulose and a completely amorphous coir cellulose; and ΔH_s , the heat required to dehydrate the sample, exposed to the same relative humidity. In this way, when ΔH_s reaches to ΔH_o , the crystallinity (CA%) approaches zero, and when ΔH_s reaches to zero, the crystallinity approaches to 100. In the absence of amorphous standard of coir fibre, we can have the qualitative value of accessibility. The broad band ($3380\text{-}3466\text{ cm}^{-1}$) is attributed to H-bonded H-O stretching⁶. Intramolecular hydrogen bonding of the hydroxyl group in the same chain of the molecule and intermolecular hydrogen bonding of the interchain provide stiffness and mechanical strength of the molecule⁷⁻⁸. The intramolecular and intermolecular bonding in a plane give order to the arrangement and crystalline structure. Ponnusamy *et al.*⁹ have also used this band for the estimation of water. Mahato *et al.*¹⁰ have used the ratio of absorption bands at 1429 cm^{-1} and 893 cm^{-1} as crystallinity index (C I) following O' Connor *et al.*¹¹ and the results have been found to be in good agreement with the measured values of crystallinity

by X-ray method. Density techniques provide an average of the packing densities of different regions with no information about the distribution or order. The chemical and sorption technique gives data dependent on both structural and chemical accessibility. Although, any technique may have some limitations, this absorption technique may prove to be very convenient for the determination of crystallinity index, which is qualitatively the opposite of amorphity. The IR spectra is the finger print of the many bonds present in the ligno - cellulosic coir fibre. IR study along with the accessibility of water sheds some light on the cross-linking, depolymerization as well as chemical and thermal degradation of the fibre. The integrated intensity of the hydroxyl band ($3380\text{-}3466\text{ cm}^{-1}$) gives the quantitative presence of the hydroxyl OH bands which can be directly measured by the area of the absorption band. OH peak location is related to the strength of the hydrogen bond involved and the stronger the hydrogen bond, the lower is the frequency of OH band¹².

3 Materials and Methods

Bristle retted fibres were cut to small pieces, combed, cleared, and then treated with different concentrations of aqueous NaOH solution from 5% to 30% w/w for three hours at each concentration at room temperature. The treated fibres were thoroughly washed with distilled water to remove alkali to obtain mercerized fibre. The treated fibres were powdered by prolong grinding in an agate mortar and pestle and finally sieved through a screen of 200 mesh. The X-ray diffractograms of the samples were recorded in a Philips X-ray diffractometer (PW 1710) covering the entire detectable range spanning between 5° (2θ) and 90° (2θ) using filtered Cu K_α radiation at 35 kV and 30 mA. IR spectra were taken by using Perkin Elmer spectrometer at 2.4 cm^{-1} . Differential scanning calorimetry (DSC) measurement was carried out by using Thermal analyzer (Simadju Model DT-40) from 20°C to 620°C at heating rate of $20^\circ\text{C}/\text{min}$ in an argon atmosphere.

4 Results and Discussion

In the raw sample, Table 1 and Fig. 1 show three consecutive distinctly separated endothermic peaks or dips in the thermogram corresponding to amorphous, para-crystalline and crystalline phases of the coir fibre³. NMR studies by Gutowsky and Pake¹³ have shown that the molecular movement in the

Table 1—DSC thermograms for different concentration of mercerization

Sample	1 st Endotherm			2 nd Endotherm			3 rd Endotherm			Energy absorbed in endotherm, mJ
	T_i °C	T_p °C	T_f °C	T_i °C	T_p °C	T_f °C	T_i °C	T_p °C	T_f °C	
Raw	20	105.2	185.1	185.1	257.3	297.8	297.8	336.7	381.2	1953.65
5% Mercerized	20	114.2	300.9	Endothermic peaks are overlapped			-	-	-	2400.3
10% Mercerized	30	111.1	228.1	288.1	-	300.3	Overlapped			2609.6
15% Mercerized	20	108.7	230.2	230.2	-	310	Overlapped			2844.8
20% Mercerized	20	105.5	239.2	239.2	-	302.3	Overlapped			3467.1
30% Mercerized	20	110	216.3	216.3	-	282	Overlapped			2222.5

T_i – Initial temperature, T_p – Peak temperature, and T_f – Final temperature.

cellulose-water system is more in non-crystalline in comparison to that in the crystalline part. The motion of the chain is rigid. This change in movement has been attributed to the intramolecular and intermolecular hydrogen bonding. The amorphous and paracrystalline components are first affected and the crystalline components are attacked at the last phase. The first broad endotherm starts from 20°C to 185.1°C, dip centered at around 105.2°C, this corresponds to the amorphous component. The second endotherm ranges from 185.1°C to 297.8°C, peak centered at 257.3°C, which corresponds to the paracrystalline distorted molecules of ligno-cellulosic material. The last endotherm starts from 297.8°C to 381.2°C, centered at around 336.7°C.

This is due to expulsion of absorbed water from the crystalline part and the structural water from the cellulose molecules. It has been reported that in ligno-cellulosic fibre such as sisal¹⁴ and wood cellulose¹⁵, the cellulose starts degrading from 310°C to 347°C. In the 5% mercerized sample, the endothermic peaks due to absorbed water in non-crystalline and crystalline region get overlapped. The 1st dehydration endothermic slightly shifts to the higher temperature 114.2°C. This increases the thermal stability of coir fibre may be due to the removal of distortion¹⁰. Saha *et al.*¹⁶ have reported that hemicellulose is removed with the alkali treatment. This overlapping or continuity of the thermogram may be because of the removal of some cross-linking in the coir fibre. At 10% mercerization, the thermogram shows overlapping of two endothermic peaks terminating at 300°C. The endothermic peak centered at around 111.1°C shifts to lower temperature which indicates the onset of the

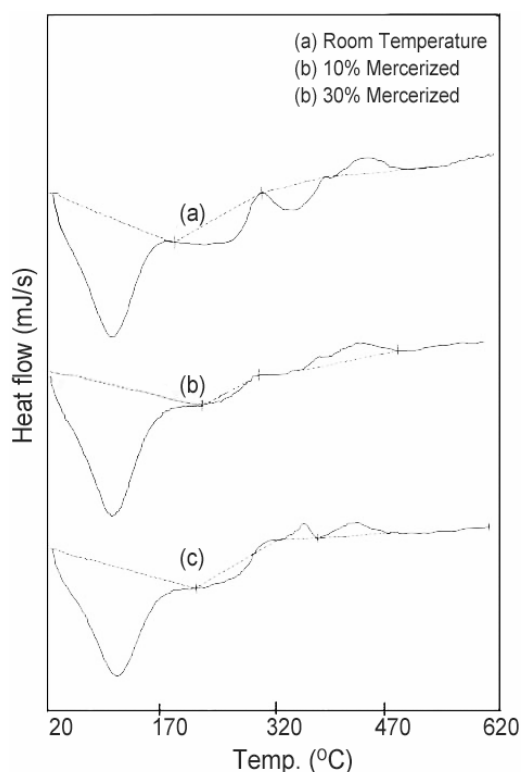


Fig. 1—Variation in DSC thermograms with concentration of mercerization

depolymerization of the ligno-cellulosic fibre. This results in the decrease in the thermal stability. At 15% mercerization along with the overlapping of the endothermic peak centered at around 108.7°C, a new exothermic peak at around 320°C appears which signifies the thermal degradation of cellulose due to oxidation. At 20% mercerization, the centre of the overlapped peak shifts towards lower temperature 105.5°C. The thermal stability is further decreased. This may be due to depolymerization of the cellulose

component¹⁷. Alkali treatment also degrades chemically hemicellulose and lignin¹⁶. This shows the lowering of the exothermic reaction centering at around 302°C. The decomposition of cellulose component in coir fibre shifts towards lower temperature. The broad and diffuse peaks show the presence of polycrystalline aggregate¹⁸. At 30% mercerization, the thermogram shows that the major portion of the endotherm is shifted towards lower temperature, which shows that as a result of alkali treatment, the major fraction of the ligno-cellulosic material has been converted into amorphous phase¹⁰. The IR spectra (Fig. 2) shows clearly the change in the H-bonded O-H band in intensity, peak position and symmetry of the absorption band. Because the coir fibre is a ligno-cellulosic complex, consisting of hemicellulose also in the basic structure, the chemical degradation of hemicellulose and lignin also affects the different absorption bands including the hydroxyl(OH) band. At 5% mercerization, the band at 1730 cm⁻¹ is missing from the spectra. The peak at 1730 cm⁻¹ is the characteristic band of carbonyl (C=O) stretching. It appears that in alkali treatment a substantial portion of uronic acid, a constituent of hemicellulose xylan, is removed resulting in the disappearance of this peak¹⁶. The crystallinity of the cellulosic fibre is also affected by the lattice transformation of native cellulose I into cellulose II. The band at 1421-1466 cm⁻¹ is attributed to both lignin and xylan due to CH₃ deformation (asymmetric) in lignin as well as CH₂ bending. Liang and Marchessault⁶ assigned the band at around 1430 cm⁻¹ to the scissoring motion of cellulose I and band at around 1420 cm⁻¹ to the cellulose II. This would imply that changes in intensity or location are related to alteration in the environment of the C₆ group including change in the hydrogen bonding. They observed that the band shifts towards lower frequency side and the intensity becomes very weak in the case of cellulose II. We have also observed the shift of the band towards the lower frequency side. However, the change in intensity observed is not so marked as is normally expected for the lattice transformation from cellulose I to cellulose II. This observation is in agreement with the XRD pattern (Fig. 3), because for cellulose II it is different. The lattice transformation is most probably restricted due to presence of lignin as mentioned earlier¹⁹. The peak at around 901 cm⁻¹ is characteristic of β -linkage and

this is assigned to C₁-H bending mode in β -linkage²⁰. The increase in intensity of this band relates to the rotation of glucose residue around the glucosidic bonds²¹ and indicates the transition from cellulose I into cellulose II. From all these considerations

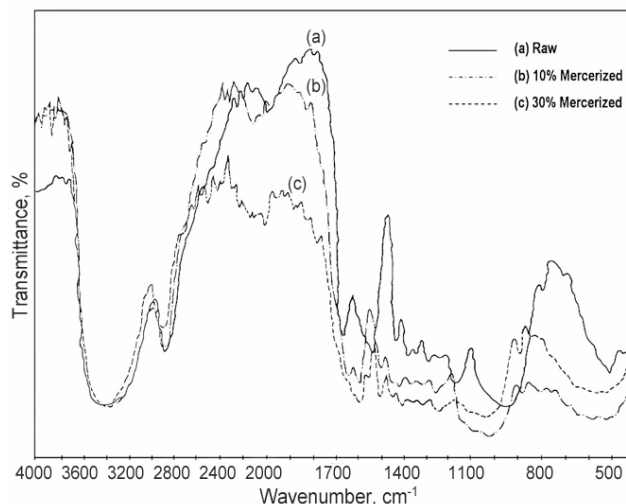


Fig. 2—Variation in IR absorption bands with concentration of mercerization

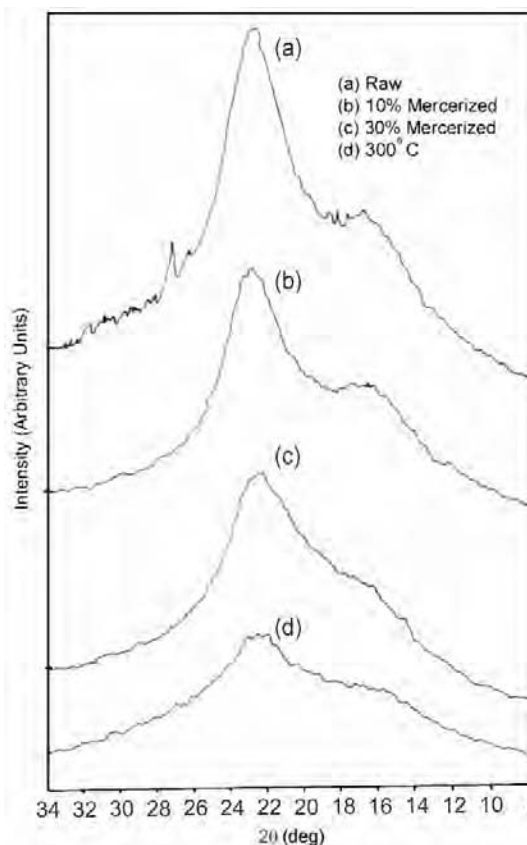


Fig. 3—Variation in XRD profiles with concentration of mercerization and temperature

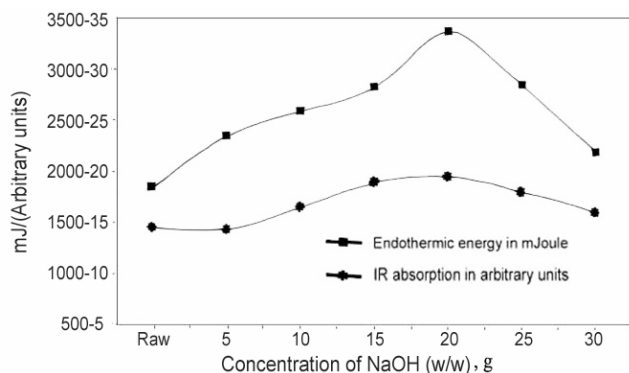


Fig. 4—Variation in accessibility (DSC & IR) with concentration of mercerization

(XRD and IR), it is obvious that lattice transformation does not take place with the mercerization of coir fibre. The semi crystalline and crystalline parts gradually convert into the amorphous phase, resulting in change in the hydroxyl(OH) band. Figure 4 shows the intensity variation of (OH) band and endothermic energy with the concentration of mercerization. The broad nature of the curves appears to match. The slight variation is due to the different methods¹⁹⁻²¹.

5 Conclusion

The accessibility increases with the amorphity of the fibre i.e. with the decrease in crystallinity of the sample. The H-bonded hydroxyl group (OH) is solely responsible for absorption of water. Water retention of the fibre is found to increase with the decrease of

crystallinity. DSC thermograms appear to support the three phase model.

References

- 1 Page D H, *Wood Fibre*, 7 (4) (1976) 246.
- 2 Mc Ginnis G D & Shafizaden F, *Pulp and Paper Chemistry and Chemical Technology*, 3rd edn, Vol. 1, edited by J P Casey (Wiley- Inter Science, New York), 1980, 1.
- 3 Mitra G B & Mukherjee P S, *Polymer*, 21 (1980) 1403.
- 4 Gardner K H & Blackwell J, *Biopolymers*, 13 (1974) 1975.
- 5 Bertran M S & Dale B E, *J Appl Polym Sci*, 32 (1986) 4241.
- 6 Liang C Y & Marchessault R H, *J Polym Sci*, 37 (1959) 385.
- 7 Jaswon M A, Gills P P & Mark R E, The elastic constants of crystalline native cellulose, *Proc Royal Soc London, Ser. A*, 306 (1968) 389.
- 8 Gills P P, *J Polym Sci*, A2, 7 (5) (1969) 783.
- 9 Ponnusamy V, Ramasamy V & Anandalakshmi K, *Indian J Pure Appl Phys*, 44 (January) (2006) 13-19.
- 10 Mahato D N, Mathur B K & Bhattacharjee S, *Indian J Phys*, 70 A (2) (1996) 203.
- 11 O' Connor R T, Dupre E F & Mitchum D, *Text Res J*, 28 (1958) 382.
- 12 Cangelosi F & Shaw M T, *Polym Eng Sci*, 23 (1983) 669.
- 13 Gutosky H S & Pake G E, *J Chem Phys*, 18 (1950) 162.
- 14 Chand N, Sood S, Singh D K & Rohatgi P K, *J Thermal Analysis*, 32 (1987) 595.
- 15 Levin E D & Belikova Z P, *Leszh*, 11 (1968) 112.
- 16 Saha S C, Das B K, Ray P K, Pandey S N & Goswami K, *J Appl Polym Sci*, 43 (1991) 1885.
- 17 Mahato D N, Prasad R N & Mathur B K, *Indian J Pure Appl Phys*, 47 (2009) 643.
- 18 Dawson P C, Gilbert M & Maddams W F, *J Polym Sci, Part B: Polym Phys*, 29 (1991) 1407.
- 19 Revol J F & Goring D A, *J Appl Polym Sci*, 26 (1981) 1275.
- 20 Barker S A, Bourne E J, Stacey M & Wifton D H, *J Chem Soc*, 171 (Part I) (1954).
- 21 Higgins H G, Goldsmith V & Mackenzie A W, *J Polym Sci*, 32 (1958) 57.